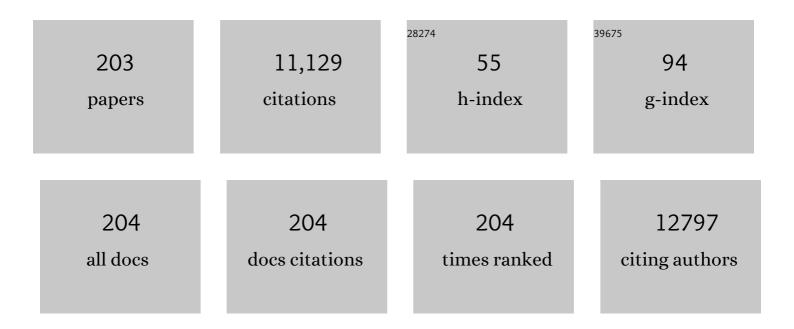
List of Publications by Year in descending order

Source: https://exaly.com/author-pdf/3378315/publications.pdf Version: 2024-02-01



#	Article	IF	CITATIONS
1	Flexible MXene-Ti3C2Tx bond few-layers transition metal dichalcogenides MoS2/C spheres for fast and stable sodium storage. Chemical Engineering Journal, 2022, 427, 130960.	12.7	15
2	Propelling the practical application of the intimate coupling of photocatalysis and biodegradation system: System amelioration, environmental influences and analytical strategies. Chemosphere, 2022, 287, 132196.	8.2	15
3	Chessboard structured electrode design for Li-S batteries Based on MXene nanosheets. Chemical Engineering Journal, 2022, 429, 131997.	12.7	15
4	MIL-47(V) catalytic conversion of H2O2 for sensitive H2O2 detection and tumor cell inhibition. Sensors and Actuators B: Chemical, 2022, 354, 131201.	7.8	19
5	Anthozoan-like porous nanocages with nano-cobalt-armed CNT multifunctional layers as a cathode material for highly stable Na–S batteries. Inorganic Chemistry Frontiers, 2022, 9, 645-651.	6.0	7
6	Ni/Li antisite induced disordered passivation layer for high-Ni layered oxide cathode material. Energy Storage Materials, 2022, 45, 720-729.	18.0	29
7	Why does the capacity of vanadium selenide based aqueous zinc ion batteries continue to increase during long cycles?. Journal of Colloid and Interface Science, 2022, 615, 30-37.	9.4	9
8	Significantly fastened redox kinetics in single crystal layered oxide cathode by gradient doping. Nano Energy, 2022, 94, 106961.	16.0	42
9	Reunderstanding the Reaction Mechanism of Aqueous Zn–Mn Batteries with Sulfate Electrolytes: Role of the Zinc Sulfate Hydroxide. Advanced Materials, 2022, 34, e2109092.	21.0	97
10	Tessellated N-doped carbon/CoSe ₂ as trap-catalyst sulfur hosts for room-temperature sodium–sulfur batteries. Inorganic Chemistry Frontiers, 2022, 9, 1743-1751.	6.0	6
11	Identification of Catalytic Active Sites for Durable Proton Exchange Membrane Fuel Cell: Catalytic Degradation and Poisoning Perspectives. Small, 2022, 18, e2106279.	10.0	25
12	Significance of gallium doping for high Ni, low Co/Mn layered oxide cathode material. Chemical Engineering Journal, 2022, 441, 135821.	12.7	34
13	A distinctive conversion mechanism for reversible zinc ion storage. Inorganic Chemistry Frontiers, 2022, 9, 2706-2713.	6.0	7
14	Carbon dots-induced carbon-coated Ni and Mo2N nanosheets for efficient hydrogen production. Electrochimica Acta, 2022, 424, 140671.	5.2	6
15	A Strategy for Polysulfides/Polyselenides Protection Based on Co ₉ S ₈ @SiO ₂ /C Host in Na‣eS ₂ Batteries. Advanced Functional Materials, 2021, 31, 2001952.	14.9	32
16	Low-operating temperature quasi-solid-state potassium-ion battery based on commercial materials. Journal of Colloid and Interface Science, 2021, 582, 932-939.	9.4	20
17	Yolk-shell porous carbon spheres@CoSe2 nanosheets as multilayer defenses system of polysulfide for advanced Li-S batteries. Chemical Engineering Journal, 2021, 413, 127521.	12.7	49
18	A new polyanionic cathode with stable structure and superior kinetics for Na-ion batteries. Chemical Engineering Journal, 2021, 405, 127035.	12.7	8

#	Article	IF	CITATIONS
19	Efficient Catalytic Conversion of Polysulfides by Biomimetic Design of "Branch-Leaf―Electrode for High-Energy Sodium–Sulfur Batteries. Nano-Micro Letters, 2021, 13, 50.	27.0	39
20	Self-Supported CdP ₂ –CDs–CoP for High-Performance OER Catalysts. ACS Sustainable Chemistry and Engineering, 2021, 9, 1297-1303.	6.7	42
21	Designing 2D nickel hydroxide@graphene nanosheet composites to confine sulfur in highly stable lithium–sulfur batteries. Sustainable Energy and Fuels, 2021, 5, 5175-5183.	4.9	1
22	Multi-step Controllable Catalysis Method for the Defense of Sodium Polysulfide Dissolution in Room-Temperature Na–S Batteries. ACS Applied Materials & Interfaces, 2021, 13, 11852-11860.	8.0	24
23	A new calcium metal organic frameworks (Ca-MOF) for sodium ion batteries. Materials Letters, 2021, 286, 129264.	2.6	24
24	Suppressed shuttling effect of polysulfides using three-dimensional nickel hydroxide polyhedrons for advanced lithium-sulfur batteries. Journal of Colloid and Interface Science, 2021, 593, 89-95.	9.4	14
25	Design of an amperometric glucose oxidase biosensor with added protective and adhesion layers. Mikrochimica Acta, 2021, 188, 312.	5.0	10
26	Heterogeneous interface designing of bimetallic selenides nanocubes for superior sodium storage. Journal of Power Sources, 2021, 506, 230249.	7.8	14
27	Gelation of organic liquid electrolyte to achieve superior sodium-ion full-cells. Journal of Colloid and Interface Science, 2021, 599, 190-197.	9.4	8
28	A self-healing neutral aqueous rechargeable Zn/MnO2 battery based on modified carbon nanotubes substrate cathode. Journal of Colloid and Interface Science, 2021, 600, 83-89.	9.4	29
29	Ultrafast kinetics and high capacity for Stable Sodium Storage enabled by Fe3Se4/ZnSe heterostructure engineering. Composites Part B: Engineering, 2021, 224, 109166.	12.0	15
30	High-rate and non-toxic Na ₇ Fe _{4.5} (P ₂ O ₇) ₄ @C for quasi-solid-state sodium-ion batteries. Materials Chemistry Frontiers, 2021, 5, 2783-2790.	5.9	3
31	A gel-limiting strategy for large-scale fabrication of Fe–N–C single-atom ORR catalysts. Journal of Materials Chemistry A, 2021, 9, 7137-7142.	10.3	51
32	A facilely-synthesized polyanionic cathode with impressive long-term cycling stability for sodium-ion batteries. Chemical Communications, 2021, 57, 9566-9569.	4.1	2
33	Lowâ€Barrier, Dendriteâ€Free, and Stable Na Plating/Stripping Enabled by Gradient Sodiophilic Carbon Skeleton. Advanced Energy Materials, 2021, 11, .	19.5	27
34	A Fe3N/carbon composite electrocatalyst for effective polysulfides regulation in room-temperature Na-S batteries. Nature Communications, 2021, 12, 6347.	12.8	71
35	Rational construction of rGO/VO2 nanoflowers as sulfur multifunctional hosts for room temperature Na-S batteries. Chemical Engineering Journal, 2020, 379, 122359.	12.7	59
36	Cobalt nanoparticles embedded into free-standing carbon nanofibers as catalyst for room-temperature sodium-sulfur batteries. Journal of Colloid and Interface Science, 2020, 565, 63-69.	9.4	34

#	Article	IF	CITATIONS
37	Puzzle-inspired carbon dots coupled with cobalt phosphide for constructing a highly-effective overall water splitting interface. Chemical Communications, 2020, 56, 257-260.	4.1	48
38	Nickel Hollow Spheres Concatenated by Nitrogenâ€Đoped Carbon Fibers for Enhancing Electrochemical Kinetics of Sodium–Sulfur Batteries. Advanced Science, 2020, 7, 1902617.	11.2	70
39	MXene-derived three-dimensional carbon nanotube network encapsulate CoS ₂ nanoparticles as an anode material for solid-state sodium-ion batteries. Journal of Materials Chemistry A, 2020, 8, 3018-3026.	10.3	51
40	Lowâ€Operating Temperature, Highâ€Rate and Durable Solid‣tate Sodiumâ€Ion Battery Based on Polymer Electrolyte and Prussian Blue Cathode. Advanced Energy Materials, 2020, 10, 1903351.	19.5	64
41	Highly efficient Fe-N-C oxygen reduction electrocatalyst engineered by sintering atmosphere. Journal of Power Sources, 2020, 449, 227497.	7.8	22
42	Hierarchical growth of vertically standing Fe3O4-FeSe/CoSe2 nano-array for high effective oxygen evolution reaction. Materials Research Bulletin, 2020, 122, 110680.	5.2	17
43	Metal chalcogenide hollow polar bipyramid prisms as efficient sulfur hosts for Na-S batteries. Nature Communications, 2020, 11, 5242.	12.8	102
44	BC@DNA-Mn ₃ (PO ₄) ₂ Nanozyme for Real-Time Detection of Superoxide from Living Cells. Analytical Chemistry, 2020, 92, 15927-15935.	6.5	18
45	CdMn Bimetallic Complex-Derived Manganese–Nitrogen Species as Electrocatalysts for an Oxygen Reduction Reaction. ACS Sustainable Chemistry and Engineering, 2020, 8, 12618-12625.	6.7	11
46	Na 3 V 2 O 2 (PO 4) 2 F Cathode for Highâ€Performance Quasiâ€Solidâ€State Sodiumâ€Ion Batteries with a Wi Workable Temperature Range. Energy Technology, 2020, 8, 2000494.	de _{3.8}	11
47	Nanoporous V-Doped Ni ₅ P ₄ Microsphere: A Highly Efficient Electrocatalyst for Hydrogen Evolution Reaction at All pH. ACS Applied Materials & Interfaces, 2020, 12, 37092-37099.	8.0	40
48	Flexible electrode constructed by encapsulating ultrafine VSe2 in carbon fiber for quasi-solid-state sodium ion batteries. Journal of Power Sources, 2020, 470, 228438.	7.8	25
49	Template method for fabricating Co and Ni nanoparticles/porous channels carbon for solid-state sodium-sulfur battery. Journal of Colloid and Interface Science, 2020, 578, 710-716.	9.4	19
50	Interfacial engineering of Ni/V2O3 for hydrogen evolution reaction. Nano Research, 2020, 13, 2407-2412.	10.4	41
51	A synergistic Bi ₂ S ₃ /MXene composite with enhanced performance as an anode material of sodium-ion batteries. New Journal of Chemistry, 2020, 44, 3072-3077.	2.8	40
52	A highly-effective nitrogen-doped porous carbon sponge electrode for advanced K–Se batteries. Inorganic Chemistry Frontiers, 2020, 7, 1182-1189.	6.0	36
53	Vanadium carbide nanoparticles incorporation in carbon nanofibers for room-temperature sodium sulfur batteries: Confining, trapping, and catalyzing. Chemical Engineering Journal, 2020, 395, 124978.	12.7	37
54	Micropore-Boosted Layered Double Hydroxide Catalysts: EIS Analysis in Structure and Activity for Effective Oxygen Evolution Reactions, ACS Applied Materials & amp: Interfaces, 2019, 11, 30887-30893.	8.0	26

#	Article	IF	CITATIONS
55	The construction of ZnS–In ₂ S ₃ nanonests and their heterojunction boosted visible-light photocatalytic/photoelectrocatalytic performance. New Journal of Chemistry, 2019, 43, 14402-14408.	2.8	12
56	MXene-derivative pompon-like Na2Ti3O7@C anode material for advanced sodium ion batteries. Chemical Engineering Journal, 2019, 378, 122209.	12.7	75
57	A labyrinth-like network electrode design for lithium–sulfur batteries. Nanoscale, 2019, 11, 14648-14653.	5.6	15
58	Jackfruit-like electrode design for advanced Na-Se batteries. Journal of Power Sources, 2019, 443, 227245.	7.8	32
59	Novel Oxygen-Deficient Zirconia (ZrO _{2–<i>x</i>}) for Fluorescence/Photoacoustic Imaging-Guided Photothermal/Photodynamic Therapy for Cancer. ACS Applied Materials & Interfaces, 2019, 11, 41127-41139.	8.0	35
60	(001) Facet-Dominated Hierarchically Hollow Na ₂ Ti ₃ O ₇ as a High-Rate Anode Material for Sodium-Ion Capacitors. ACS Applied Materials & Interfaces, 2019, 11, 42197-42205.	8.0	31
61	Design and Construction of Sodium Polysulfides Defense System for Roomâ€Temperature Na–S Battery. Advanced Science, 2019, 6, 1901557.	11.2	106
62	A rough endoplasmic reticulum-like VSe ₂ /rGO anode for superior sodium-ion capacitors. Inorganic Chemistry Frontiers, 2019, 6, 2935-2943.	6.0	46
63	A railway-like network electrode design for room temperature Na–S battery. Journal of Materials Chemistry A, 2019, 7, 150-156.	10.3	60
64	Preparation of MoS ₂ /Ti ₃ C ₂ T _x composite as anode material with enhanced sodium/lithium storage performance. Inorganic Chemistry Frontiers, 2019, 6, 117-125.	6.0	59
65	Novel CdFe Bimetallic Complex-Derived Ultrasmall Fe- and N-Codoped Carbon as a Highly Efficient Oxygen Reduction Catalyst. ACS Applied Materials & Interfaces, 2019, 11, 21481-21488.	8.0	21
66	Double-walled N-doped carbon@NiCo ₂ S ₄ hollow capsules as SeS ₂ hosts for advanced Li–SeS ₂ batteries. Journal of Materials Chemistry A, 2019, 7, 12276-12282.	10.3	40
67	Constructing high effective nano-Mn3(PO4)2-chitosan in situ electrochemical detection interface for superoxide anions released from living cell. Biosensors and Bioelectronics, 2019, 133, 133-140.	10.1	29
68	TiOxNy nanoparticles/C composites derived from MXene as anode material for potassium-ion batteries. Chemical Engineering Journal, 2019, 369, 828-833.	12.7	68
69	Amorphous nickel sulfide nanosheets with embedded vanadium oxide nanocrystals on nickel foam for efficient electrochemical water oxidation. Journal of Materials Chemistry A, 2019, 7, 10534-10542.	10.3	65
70	Facile and Scale Synthesis of Co/N/S-Doped Porous Graphene-Like Carbon Architectures as Electrocatalysts for Sustainable Zinc-Air Battery Cells. ACS Sustainable Chemistry and Engineering, 2019, 7, 7743-7749.	6.7	24
71	A coaxial nanocable textured by a cerium oxide shell and carbon core for sensing nitric oxide. Mikrochimica Acta, 2019, 186, 789.	5.0	1
72	Nitrogenâ€Doped Carbon as a Host for Tellurium for Highâ€Rate Li–Te and Na–Te Batteries. ChemSusChem, 2019, 12, 1196-1202.	6.8	18

#	Article	IF	CITATIONS
73	High-Rate and Long-Life Sodium-Ion Batteries Based on Sponge-like Three-Dimensional Porous Na-Rich Ferric Pyrophosphate Cathode Material. ACS Applied Materials & Interfaces, 2019, 11, 5107-5113.	8.0	30
74	†Circuit board-like CoS/MXene composite with superior performance for sodium storage. Chemical Engineering Journal, 2019, 357, 220-225.	12.7	143
75	MoP nanoparticles with a P-rich outermost atomic layer embedded in N-doped porous carbon nanofibers: Self-supported electrodes for efficient hydrogen generation. Nano Research, 2018, 11, 4728-4734.	10.4	59
76	Interface engineered construction of porous g-C3N4/TiO2 heterostructure for enhanced photocatalysis of organic pollutants. Applied Surface Science, 2018, 440, 229-236.	6.1	58
77	Honeycombâ€Like Spherical Cathode Host Constructed from Hollow Metallic and Polar Co ₉ S ₈ Tubules for Advanced Lithium–Sulfur Batteries. Advanced Functional Materials, 2018, 28, 1704443.	14.9	236
78	FePO4 embedded in nanofibers consisting of amorphous carbon and reduced graphene oxide asÂan enzyme mimetic for monitoring superoxide anions released by living cells. Mikrochimica Acta, 2018, 185, 140.	5.0	27
79	Nanosized Metal Phosphides Embedded in Nitrogenâ€Đoped Porous Carbon Nanofibers for Enhanced Hydrogen Evolution at All pH Values. Angewandte Chemie, 2018, 130, 1981-1985.	2.0	58
80	Improving the Performance of Hard Carbon//Na ₃ V ₂ O ₂ (PO ₄) ₂ F Sodium-Ion Full Cells by Utilizing the Adsorption Process of Hard Carbon. ACS Applied Materials & Interfaces, 2018, 10, 16581-16587.	8.0	37
81	An iron hydroxyl phosphate microoctahedron catalyst as an efficient peroxidase mimic for sensitive and colorimetric quantification of H ₂ O ₂ and glucose. New Journal of Chemistry, 2018, 42, 6803-6809.	2.8	15
82	Synthesis of M (Fe3C, Co, Ni)-porous carbon frameworks as high-efficient ORR catalysts. Energy Storage Materials, 2018, 11, 112-117.	18.0	71
83	Ultrafine TiO2 encapsulated in nitrogen-doped porous carbon framework for photocatalytic degradation of ammonia gas. Chemical Engineering Journal, 2018, 331, 383-388.	12.7	44
84	Nanosized Metal Phosphides Embedded in Nitrogenâ€Doped Porous Carbon Nanofibers for Enhanced Hydrogen Evolution at All pH Values. Angewandte Chemie - International Edition, 2018, 57, 1963-1967.	13.8	277
85	Muscle-like electrode design for Li-Te batteries. Energy Storage Materials, 2018, 10, 10-15.	18.0	40
86	Efficient in situ growth of enzyme-inorganic hybrids on paper strips for the visual detection of glucose. Biosensors and Bioelectronics, 2018, 99, 603-611.	10.1	56
87	An excellent full sodium-ion capacitor derived from a single Ti-based metal–organic framework. Journal of Materials Chemistry A, 2018, 6, 24860-24868.	10.3	33
88	Self-Supported FeCo ₂ S ₄ Nanotube Arrays as Binder-Free Cathodes for Lithium–Sulfur Batteries. ACS Applied Materials & Interfaces, 2018, 10, 43707-43715.	8.0	75
89	Chinese knot-like electrode design for advanced Li-S batteries. Nano Energy, 2018, 53, 354-361.	16.0	72
90	Double‣helled NiOâ€NiCo ₂ O ₄ Heterostructure@Carbon Hollow Nanocages as an Efficient Sulfur Host for Advanced Lithium–Sulfur Batteries. Advanced Energy Materials, 2018, 8, 1800709.	19.5	236

#	Article	IF	CITATIONS
91	Mesoporous Hollow Nitrogen-Doped Carbon Nanospheres with Embedded MnFe ₂ O ₄ /Fe Hybrid Nanoparticles as Efficient Bifunctional Oxygen Electrocatalysts in Alkaline Media. ACS Applied Materials & Interfaces, 2018, 10, 20440-20447.	8.0	73
92	Metal-organic complex derived hierarchical porous carbon as host matrix for rechargeable Na-Se batteries. Electrochimica Acta, 2018, 276, 21-27.	5.2	28
93	Engineering the nanostructure of molybdenum nitride nanodot embedded N-doped porous hollow carbon nanochains for rapid all pH hydrogen evolution. Journal of Materials Chemistry A, 2018, 6, 14734-14741.	10.3	56
94	Potassium titanium hexacyanoferrate as a cathode material for potassium-ion batteries. Journal of Physics and Chemistry of Solids, 2018, 122, 31-35.	4.0	43
95	Controlled synthesis of Mn3(PO4)2 hollow spheres as biomimetic enzymes for selective detection of superoxide anions released by living cells. Mikrochimica Acta, 2017, 184, 1177-1184.	5.0	22
96	Cobalt nanoparticle decorated graphene aerogel for efficient oxygen reduction reaction electrocatalysis. International Journal of Hydrogen Energy, 2017, 42, 5930-5937.	7.1	28
97	Ternary Ni _{<i>x</i>} Co _{3â^'<i>x</i>} S ₄ with a Fine Hollow Nanostructure as a Robust Electrocatalyst for Hydrogen Evolution. ChemCatChem, 2017, 9, 4169-4174.	3.7	18
98	Uniform α-Ni(OH)2 hollow spheres constructed from ultrathin nanosheets as efficient polysulfide mediator for long-term lithium-sulfur batteries. Energy Storage Materials, 2017, 8, 202-208.	18.0	93
99	Design and fabrication of highly sensitive and stable biochip for glucose biosensing. Applied Surface Science, 2017, 422, 900-904.	6.1	14
100	Confined selenium within metal-organic frameworks derived porous carbon microcubes as cathode for rechargeable lithium–selenium batteries. Journal of Power Sources, 2017, 341, 53-59.	7.8	56
101	Synthesis of Cobalt Phosphide Nanoparticles Supported on Pristine Graphene by Dynamically Selfâ€Assembled Graphene Quantum Dots for Hydrogen Evolution. ChemSusChem, 2017, 10, 1014-1021.	6.8	42
102	Porous carbon derived from Sunflower as a host matrix for ultra-stable lithium–selenium battery. Journal of Colloid and Interface Science, 2017, 490, 747-753.	9.4	22
103	Investigation of Fe ₂ N@carbon encapsulated in N-doped graphene-like carbon as a catalyst in sustainable zinc–air batteries. Catalysis Science and Technology, 2017, 7, 5670-5676.	4.1	56
104	Design and synthesis of Co–N–C porous catalyst derived from metal organic complexes for highly effective ORR. Dalton Transactions, 2017, 46, 15646-15650.	3.3	44
105	Assembling Hollow Cobalt Sulfide Nanocages Array on Graphene-like Manganese Dioxide Nanosheets for Superior Electrochemical Capacitors. ACS Applied Materials & Interfaces, 2017, 9, 35040-35047.	8.0	107
106	Three-dimensional hierarchical porous tubular carbon as a host matrix for long-term lithium-selenium batteries. Journal of Power Sources, 2017, 367, 17-23.	7.8	28
107	Design, synthesis and photodegradation ammonia properties of MoS2@TiO2 encapsulated carbon coaxial nanobelts. Materials Letters, 2017, 209, 56-59.	2.6	14
108	Ascorbic acid-tailored synthesis of carbon-wrapped nanocobalt encapsulated in graphene aerogel as electrocatalysts for highly effective oxygen-reduction reaction. Journal of Solid State Electrochemistry, 2017, 21, 3641-3648.	2.5	6

#	Article	IF	CITATIONS
109	Hollow Co ₃ O ₄ Nanocages Decorated Graphene Aerogels Derived from Carbon Wrapped Nanoâ€Co for Efficient Oxygen Reduction Reaction. ChemistrySelect, 2017, 2, 6359-6363.	1.5	6
110	Analysis of graphene-like activated carbon derived from rice straw for application in supercapacitor. Chinese Chemical Letters, 2017, 28, 2290-2294.	9.0	51
111	Biomass-derived synthesis of nitrogen and phosphorus Co-doped mesoporous carbon spheres as catalysts for oxygen reduction reaction. Journal of Solid State Electrochemistry, 2017, 21, 103-110.	2.5	23
112	Nanostructured cobalt phosphates as excellent biomimetic enzymes to sensitively detect superoxide anions released from living cells. Biosensors and Bioelectronics, 2017, 87, 998-1004.	10.1	59
113	Three-dimensional nanotubes composed of carbon-anchored ultrathin MoS ₂ nanosheets with enhanced lithium storage. Physical Chemistry Chemical Physics, 2016, 18, 19792-19797.	2.8	18
114	Bismuth oxychloride ultrathin nanoplates as an anode material for sodium-ion batteries. Materials Letters, 2016, 178, 44-47.	2.6	32
115	Tuning and thermal exfoliation graphene-like carbon nitride nanosheets for superior photocatalytic activity. Ceramics International, 2016, 42, 18521-18528.	4.8	82
116	In situ synthesis and analytical investigation of porous Hb–Mn3(PO4)2 hybrid nanosheets and their biosensor applications. RSC Advances, 2016, 6, 95199-95203.	3.6	8
117	Nanocubic KTi ₂ (PO ₄) ₃ electrodes for potassium-ion batteries. Chemical Communications, 2016, 52, 11661-11664.	4.1	189
118	Bimetal–organic-frameworks-derived yolk–shell-structured porous Co ₂ P/ZnO@PC/CNTs hybrids for highly sensitive non-enzymatic detection of superoxide anion released from living cells. Chemical Communications, 2016, 52, 12442-12445.	4.1	22
119	Exploration of a calcium–organic framework as an anode material for sodium-ion batteries. Chemical Communications, 2016, 52, 9969-9971.	4.1	29
120	Platanus hispanica-inspired design of Co–carbon nanotube frameworks through chemical vapor deposition: a highly integrated hierarchical electrocatalyst for oxygen reduction reactions. Chemical Communications, 2016, 52, 12992-12995.	4.1	13
121	Evaluation of O3-type Na0.8Ni0.6Sb0.4O2 as cathode materials for sodium-ion batteries. Journal of Solid State Electrochemistry, 2016, 20, 2331-2335.	2.5	9
122	Aspergillus flavus Conidia-derived Carbon/Sulfur Composite as a Cathode Material for High Performance Lithium–Sulfur Battery. Scientific Reports, 2016, 6, 18739.	3.3	22
123	Selenium Embedded in Metal–Organic Framework Derived Hollow Hierarchical Porous Carbon Spheres for Advanced Lithium–Selenium Batteries. ACS Applied Materials & Interfaces, 2016, 8, 16063-16070.	8.0	106
124	NiMoO4 nanofibres designed by electrospining technique for glucose electrocatalytic oxidation. Analytica Chimica Acta, 2016, 905, 72-78.	5.4	72
125	Ni(II)-Based Metal-Organic Framework Anchored on Carbon Nanotubes for Highly Sensitive Non-Enzymatic Hydrogen Peroxide Sensing. Electrochimica Acta, 2016, 190, 365-370.	5.2	144
126	Nanostring-cluster hierarchical structured Bi ₂ O ₃ : synthesis, evolution and application in biosensing. Physical Chemistry Chemical Physics, 2016, 18, 1931-1936.	2.8	9

#	Article	IF	CITATIONS
127	Carbon nanotubes implanted manganese-based MOFs for simultaneous detection of biomolecules in body fluids. Analyst, The, 2016, 141, 1279-1285.	3.5	62
128	Analysis of cobalt phosphide (CoP) nanorods designed for non-enzyme glucose detection. Analyst, The, 2016, 141, 256-260.	3.5	83
129	Electrospinning Synthesis of Porous CoWO ₄ Nanofibers as an Ultrasensitive, Nonenzymatic, Hydrogenâ€Peroxideâ€Sensing Interface with Enhanced Electrocatalysis. ChemElectroChem, 2015, 2, 2061-2070.	3.4	15
130	3D interpenetrating macroporous graphene aerogels with MnO2 coating for supercapacitors. Russian Journal of Electrochemistry, 2015, 51, 782-788.	0.9	6
131	Bioinspired synthesis of nitrogen/sulfur co-doped graphene as an efficient electrocatalyst for oxygen reduction reaction. Journal of Power Sources, 2015, 279, 252-258.	7.8	117
132	pH-controllable synthesis of unique nanostructured tungsten oxide aerogel and its sensitive glucose biosensor. Nanotechnology, 2015, 26, 115602.	2.6	18
133	Photocatalytic activity of Pt-modified Bi2WO6 nanoporous wall under sunlight. Journal of Nanoparticle Research, 2015, 17, 1.	1.9	12
134	Na _{3.12} Fe _{2.44} (P ₂ O ₇) ₂ /multi-walled carbon nanotube composite as a cathode material for sodium-ion batteries. Journal of Materials Chemistry A, 2015, 3, 17224-17229.	10.3	74
135	Porous graphene to encapsulate Na _{6.24} Fe _{4.88} (P ₂ O ₇) ₄ as composite cathode materials for Na-ion batteries. Chemical Communications, 2015, 51, 13120-13122.	4.1	51
136	A 3D porous interconnected NaVPO ₄ F/C network: preparation and performance for Na-ion batteries. RSC Advances, 2015, 5, 40065-40069.	3.6	39
137	In situ growth of metallic silver on glucose oxidase for a highly sensitive glucose sensor. RSC Advances, 2015, 5, 34486-34490.	3.6	9
138	In situ synthesis and excellent photocatalytic activity of tiny Bi decorated bismuth tungstate nanorods. RSC Advances, 2015, 5, 85500-85505.	3.6	17
139	Experimental investigation of the important influence of pretreatment process of thermally exfoliated graphene on their microstructure and supercapacitor performance. Electrochimica Acta, 2015, 180, 187-195.	5.2	11
140	A selenium-confined porous carbon cathode from silk cocoons for Li–Se battery applications. RSC Advances, 2015, 5, 96146-96150.	3.6	24
141	A facile and well-tailored vanadium oxide porous network for high-capacity electrochemical capacitive energy storage. Materials Letters, 2014, 120, 283-286.	2.6	13
142	Design and synthesis of carbonized polypyrrole-coated graphene aerogel acting as an efficient metal-free catalyst for oxygen reduction. RSC Advances, 2014, 4, 16979-16984.	3.6	24
143	MnO ₂ -assisted fabrication of PANI/MWCNT composite and its application as a supercapacitor. RSC Advances, 2014, 4, 33569-33573.	3.6	28
144	An architectural development for energy conversion materials: morphology-conserved transformation synthesis of manganese oxides and their application in lithium ion batteries. Journal of Materials Chemistry A, 2014, 2, 3749.	10.3	31

#	Article	IF	CITATIONS
145	Synthesis and application of ultra-long Na _{0.44} MnO ₂ submicron slabs as a cathode material for Na-ion batteries. RSC Advances, 2014, 4, 38140-38143.	3.6	57
146	Synthesis of sodium manganese oxides with tailored multi-morphologies and their application in lithium/sodium ion batteries. RSC Advances, 2014, 4, 30340.	3.6	10
147	Self-assembled hierarchical graphene/polyaniline hybrid aerogels for electrochemical capacitive energy storage. Electrochimica Acta, 2014, 137, 381-387.	5.2	82
148	Multimodal porous CNT@TiO2 nanocables with superior performance in lithium-ion batteries. Journal of Materials Chemistry A, 2013, 1, 8525.	10.3	59
149	Effect of alkaline and alkaline–earth cations on the supercapacitor performance of MnO2 with various crystallographic structures. Journal of Solid State Electrochemistry, 2013, 17, 1357-1368.	2.5	27
150	Self-assembly of three-dimensional interconnected graphene-based aerogels and its application in supercapacitors. Journal of Colloid and Interface Science, 2013, 407, 416-424.	9.4	111
151	A green and facile route for constructing flower-shaped TiO ₂ nanocrystals assembled on graphene oxide sheets for enhanced photocatalytic activity. Nanotechnology, 2013, 24, 275602.	2.6	23
152	Self-assembled three-dimensional interpenetrating porous graphene aerogels with MnO2 coating and their application as high-performance supercapacitors. New Journal of Chemistry, 2013, 37, 4199.	2.8	20
153	Environmentally-friendly biomimicking synthesis of TiO2 nanomaterials using saccharides to tailor morphology, crystal phase and photocatalytic activity. CrystEngComm, 2013, 15, 4694.	2.6	22
154	Self-assembled three-dimensional graphene/OMCs hybrid aerogels for high-rate supercapacitive energy storage. RSC Advances, 2013, 3, 25317.	3.6	8
155	Nitrogen-doped reduced-graphene oxide as an efficient metal-free electrocatalyst for oxygen reduction in fuel cells. RSC Advances, 2013, 3, 3990.	3.6	112
156	Effective microwave-assisted synthesis of graphenenanosheets/NiO composite for high-performance supercapacitors. New Journal of Chemistry, 2013, 37, 439-443.	2.8	34
157	Effects of Reaction Temperature on Microstructure and Advanced Pseudocapacitor Properties of NiO Prepared via Simple Precipitation Method. Nano-Micro Letters, 2013, 5, 289-295.	27.0	14
158	Plastic protein microarray to investigate the molecular pathways of magnetic nanoparticle-induced nanotoxicity. Nanotechnology, 2013, 24, 175501.	2.6	28
159	Synthesis and photoluminescence of Eu2+ by co-doping Eu3+ and Clâ^' in Sr2P2O7 under air atmosphere. Journal of Alloys and Compounds, 2012, 512, 323-327.	5.5	37
160	Environment-friendly biomimetic synthesis of TiO ₂ nanomaterials for photocatalytic application. Nanotechnology, 2012, 23, 205601.	2.6	44
161	Flower-like NiO structures: Controlled hydrothermal synthesis and electrochemical characteristic. Materials Research Bulletin, 2012, 47, 3947-3951.	5.2	29
162	A facile route for constructing a graphene-chitosan-ZrO2 composite for direct electron transfer and glucose sensing. RSC Advances, 2012, 2, 8172.	3.6	44

#	Article	IF	CITATIONS
163	One step microwave synthesis and magnetic properties of Co3O4 octahedrons. Materials Letters, 2012, 83, 195-197.	2.6	19
164	Rapid synthesis of Mn3O4 by in-situ redox method and its capacitive performances. Rare Metals, 2011, 30, 81-84.	7.1	18
165	Synthesis and electrochemical properties of nanosized carbon-coated Li1â^'3x La x FePO4 composites. Journal of Solid State Electrochemistry, 2010, 14, 889-895.	2.5	18
166	Facile synthesis of Ag/ZnO nanorods using Ag/C cables as templates and their gas-sensing properties. Materials Letters, 2010, 64, 243-245.	2.6	48
167	Novel mesoporous MnO2 for high-rate electrochemical capacitive energy storage. Electrochimica Acta, 2010, 55, 5117-5122.	5.2	68
168	Electrocatalysis in microbial fuel cells—from electrode material to direct electrochemistry. Energy and Environmental Science, 2010, 3, 544.	30.8	225
169	Synthesis and electrochemical properties of nanostructured LiAl x Mn2 â^' x O4 â^' y Br y partic of Solid State Electrochemistry, 2009, 13, 799-805.	cles. Journa 2.5	^{al} 20
170	LiMn2O4–yBr y Nanoparticles Synthesized by a Room Temperature Solid-State Coordination Method. Nanoscale Research Letters, 2009, 4, 353-358.	5.7	18
171	Preparation and characterization of novel spinel Li4Ti5O12â^'xBrx anode materials. Electrochimica Acta, 2009, 54, 4772-4776.	5.2	175
172	Biomolecule-assisted synthesis of cobalt sulfide nanowires for application in supercapacitors. Journal of Power Sources, 2008, 180, 676-681.	7.8	315
173	Template-Free Electrochemical Synthesis of Superhydrophilic Polypyrrole Nanofiber Network. Macromolecules, 2008, 41, 7053-7057.	4.8	135
174	Shape Evolution and Magnetic Properties of Cobalt Sulfide. Crystal Growth and Design, 2008, 8, 3745-3749.	3.0	123
175	Well-Aligned Cone-Shaped Nanostructure of Polypyrrole/RuO ₂ and Its Electrochemical Supercapacitor. Journal of Physical Chemistry C, 2008, 112, 14843-14847.	3.1	231
176	Supercapacitance of Solid Carbon Nanofibers Made from Ethanol Flames. Journal of Physical Chemistry C, 2008, 112, 3612-3618.	3.1	83
177	New Nanostructured TiO ₂ for Direct Electrochemistry and Glucose Sensor Applications. Advanced Functional Materials, 2008, 18, 591-599.	14.9	416
178	Nanostructured Polyaniline/Titanium Dioxide Composite Anode for Microbial Fuel Cells. ACS Nano, 2008, 2, 113-119.	14.6	381
179	Lithium Insertion in Channel-Structured β-AgVO ₃ : <i>In Situ</i> Raman Study and Computer Simulation. Chemistry of Materials, 2007, 19, 5965-5972.	6.7	37
180	Preparation of hexagonal nanoporous nickel hydroxide film and its application for electrochemical capacitor. Electrochemistry Communications, 2007, 9, 869-874.	4.7	279

#	Article	IF	CITATIONS
181	Novel porous anatase TiO2 nanorods and their high lithium electroactivity. Electrochemistry Communications, 2007, 9, 1233-1238.	4.7	112
182	Carbon nanotube/polyaniline composite as anode material for microbial fuel cells. Journal of Power Sources, 2007, 170, 79-84.	7.8	564
183	Synthesis and Electrical Transport of Novel Channel-Structuredβ-AgVO3. Small, 2007, 3, 1174-1177.	10.0	82
184	Nanocrystalline nickel cobalt hydroxides/ultrastable Y zeolite composite for electrochemical capacitors. Journal of Solid State Electrochemistry, 2007, 11, 571-576.	2.5	71
185	Mesoporous amorphous MnO2 as electrode material for supercapacitor. Journal of Solid State Electrochemistry, 2007, 11, 1101-1107.	2.5	187
186	Preparation and electrochemical properties of LiMn2O4 by the microwave-assisted rheological phase method. Electrochimica Acta, 2007, 52, 3286-3293.	5.2	19
187	Morphology and electrochemistry of LiMn2O4 optimized by using different Mn-sources. Journal of Power Sources, 2007, 164, 885-889.	7.8	54
188	Synthesis and electrochemical properties of LiAl0.05Mn1.95O4 by the ultrasonic assisted rheological phase method. Electrochimica Acta, 2006, 51, 4701-4708.	5.2	40
189	Synthesis and electrochemical properties of LiAl0.1Mn1.9O4 by microwave-assisted sol–gel method. Journal of Power Sources, 2006, 154, 239-245.	7.8	49
190	Highly ordered MnO2 nanowire array thin films on Ti/Si substrate as an electrode for electrochemical capacitor. Journal of Solid State Chemistry, 2006, 179, 1351-1355.	2.9	70
191	A series of spinel phase cathode materials prepared by a simple hydrothermal process for rechargeable lithium batteries. Journal of Solid State Chemistry, 2006, 179, 2133-2140.	2.9	9
192	Synthesis and electrochemical properties of chemically substituted LiMn2O4 prepared by a solution-based gel method. Journal of Colloid and Interface Science, 2006, 300, 633-639.	9.4	28
193	Synthesis and electrochemical properties of spinel LiMn2O4 prepared by the rheological phase method. Journal of Solid State Electrochemistry, 2006, 10, 277-282.	2.5	8
194	Enhancement of the electrochemical properties of LiMn2O4 through chemical substitution. Materials Chemistry and Physics, 2006, 95, 188-192.	4.0	18
195	Hydrothermal synthesis of single-crystal VO2(B) nanobelts. Materials Research Bulletin, 2006, 41, 1985-1989.	5.2	27
196	Electrochemical properties and synthesis of LiAl0.05Mn1.95O3.95F0.05 by a solution-based gel method for lithium secondary battery. Journal of Solid State Chemistry, 2005, 178, 897-901.	2.9	18
197	Enhanced photocatalytic activity of magnetic TiO2 photocatalyst by silver deposition. Materials Letters, 2005, 59, 2194-2198.	2.6	75
198	Synthesis and electrochemical properties of LiMn2O4 by microwave-assisted sol–gel method. Materials Letters, 2005, 59, 3761-3765.	2.6	29

#	Article	IF	CITATIONS
199	Synthesis and electrochemical characterization of amorphous MnO2 for electrochemical capacitor. Materials Science & Engineering A: Structural Materials: Properties, Microstructure and Processing, 2005, 397, 305-309.	5.6	74
200	Enhancement of the electrochemical properties of LiMn2O4 through Al3+ and Fâ^' co-substitution. Journal of Colloid and Interface Science, 2005, 291, 433-437.	9.4	22
201	Influence of cation (NH4+) on electrochemical characteristics of MnO2 nanowire synthesized by hydrothermal method. Journal of Solid State Electrochemistry, 2005, 9, 655-659.	2.5	8
202	One-Step, Low-Temperature Route for the Preparation of Spinel LiMn[sub 2]O[sub 4] as a Cathode Material for Rechargeable Lithium Batteries. Journal of the Electrochemical Society, 2005, 152, A2030.	2.9	26
203	Bacterial cellulose network based gel polymer electrolyte for quasi-solid-state sodium-ion battery. Journal of Materials Science: Materials in Electronics, 0, , .	2.2	1